Sub Topic: e.g. Laminar Flames

Spring Technical Meeting
Eastern States Section of the Combustion Institute
March 6-9, 2022
Orlando, Florida

Experimental and computational study of droplet-shockwave interaction for pure fluids and nanofluids

James Leung[*1], *Mohana Gurunadhan*[1], *Shyam Menon*[1]

[1]*Mechanical and Industrial Engineering Department, Louisiana State University, Baton Rouge, LA 70803*
[*]*Corresponding Author Email: jleung3@lsu.edu*

Abstract: The interaction between a propagating shock wave with droplets forms a fundamental process occurring in several propulsion applications. The ensuing processes including droplet aero-breakup and vaporization for non-reacting fluids, as well as ignition and heat release for reacting fluid, are strongly influenced by the droplet-shock wave interaction. The underlying physics can be further influenced by the presence of nanoparticles in the fluids as is the case for energetic fuels. This study will consider the droplet-shock wave interaction for non-reacting fluids with and without nanoparticles. A shock wave generated into the ambient by a pressurized tube is impacted upon single droplets suspended using an acoustic levitator. The subsequent droplet breakup, and acceleration of the dispersed droplet mass is studied using high-speed imaging including a Schlieren-based approach. Tests are conducted for droplets with and without nanoparticles, and effects of varying shock speed and strength are evaluated by studying the breakup and acceleration processes. Measurement results are compared with numerical simulations of the breakup phenomena conducted using Ansys FLUENT. The simulations model the problem using both a 2-D planar approach and a 3-D periodic boundary approach and utilize the Volume-of-Fluid technique for interface capture. Measurements of droplet mass loss and centroid motion will be directly compared with simulation results. Overall, the study will provide insight into the complex multiphase physics involved in droplet-shock wave interaction processes.
Keywords: Aerobreakup, Shockwave, Droplet, Nanofluid

1. Introduction

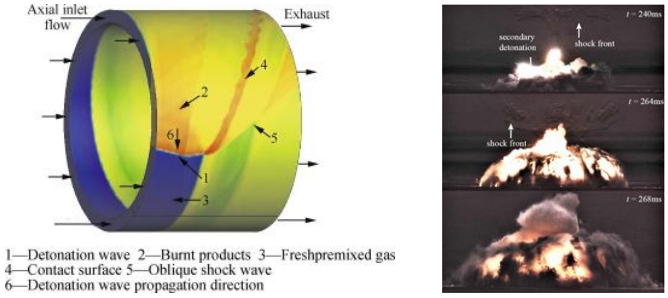

Figure 1. Configurations involving droplet-shock wave interactions: Flow Phenomena in RDE [1]; Fuel droplet explosions [2]

The interaction of a propagating shock wave with liquid droplets leading to their subsequent aerobreakup has application in various fields including rain droplets impinging on aircraft in high-speed flight [3] and two-phase detonations [2]. Another application of current interest is the consideration of liquid spray injection into rotating detonation engines (RDE's) [1] such as the one

illustrated in Fig. 1. Spray aerobreakup through the influence of a moving shock wave should have a controlling effect on ignition processes for an RDE operating on liquid fuels.

A number of researchers have considered droplet-shock wave interactions utilizing experimental and computational approaches [4, 5]. Regimes of droplet aerobreakup at high density ratios and Reynolds numbers have been classified in previous work [6] on the basis of Weber numbers ($We = \rho_g D_0 u_\infty / \gamma$) and the Ohnesorge number ($Oh = v_l / \sqrt{\rho_l D_0 \gamma}$). The extended implication of this observation is that in the case of liquid fuels where atomization precedes ignition, the dependence of fluid properties and subsequently the *We* and *Oh* numbers on combustion processes initiated by droplet aerobreakup needs to be fully characterized.

Nanoparticles offer an opportunity to increase the energy density of the fuel. This strategy has been investigated in several previous works in the context of combustion in gas turbine combustors, rocket engines, and diesel engines. Various nanoparticles such as Boron [7] and Alumina [8] have been considered as an additive for conventional liquid fuels.

Based on the preceding discussion, the broader goals of this work are to examine the issue of fuel droplet ignition following aerobreakup in the context of We and Oh numbers for liquid fuels comprising pure fluid and nanofluid droplets. In the current work, an experimental setup utilizing a shock generating pressurized tube is used with a droplet levitation system to investigate droplet-shockwave interaction. Details of the experimental setup, diagnostics, and experimental procedure are discussed. Results obtained using high-speed imaging using conventional and Schlieren approaches for pure fluid and nanofluid droplets are analyzed and discussed. Complementary multiphase numerical simulations used to study the observed experimental configuration are discussed. Experimental and computational results are used to analyze features of the droplet breakup process and conclusions are presented.

2. Methods

2.1 Experiment

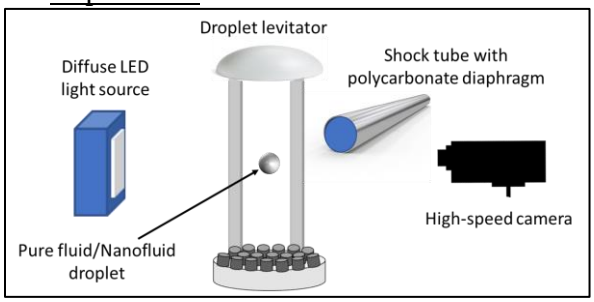

Figure 2. Experimental Setup

Figure 2 shows the experimental setup. It consists of a miniature shock-generating tube. The tube is constructed using pipe sections where a high pressure section connects to a compressed air cylinder. The high pressure section is separated from a low pressure section by an electrically actuated solenoid valve. A polycarbonate diaphragm is located at the end of the low-pressure section. To generate a shock wave, a diaphragm is installed in place. The high-pressure end is filled with air to the required driver pressure. Once the solenoid is activated, the high pressure air rushes into the low pressure section. This results in the diaphragm expanding outwards and eventually bursting. The shock wave and subsequent high speed flow generated by the bursting of the diaphragm is directed towards a droplet kept levitated using an acoustic levitator. A 3D printed single-axis acoustic levitator [TinyLev] consists of an array of ultrasonic emitters installed on mirroring top and bottom curved surfaces. This system with a total of 72 transducers whose location and inclination are selected such that they focus their energies towards a single point. The transducers are controlled using input generated by an Arduino Nano and operates at a frequency of 40 kHz. Droplets of the fluid to be tested are levitated in the levitator module prior to generating the shock wave. Best results are obtained by dispensing the fluid using a syringe fitted with a

needle tip. It is found difficult to accurately control the size of the droplet but typical droplet size ranges from 1.5-2.7 mm. Observations of the shock generated by the setup and the droplet breakup process are conducted using high-speed imaging. A high-speed camera (Photron SA-3) is used with a diffuse light source to captur images of the droplet breakup process. Imaging was carried out at 20 kfps with a resolution of 512x128 pixels. Pixel size is estimated to be 141.58 mu.m. The camera is triggered manually synchronized with the opening of the solenoid valve. Visualization of the shock structures and high speed flows behind the shock front are acquired using high-speed Schlieren imaging using a traditional Z-type Schlieren setup as shown in Fig. 2. The setup consists of two 6" mirrors of 60" focal length where a controllable light source is placed at the focal length of one of the mirrors. The camera is focused upon the droplets levitated in the test section. Tests were conducted using three fluids, water, aluminum oxide (Al2O3) nanofluid, and titanium dioxide (TiO2) nanofluid. Al2O3 nanofluid consisted of spherical Al2O3 nanoparticles, 30 nm in diameter, 20 wt% dispersed in water. TiO2 nanofluid consisted of spherical TiO2 nanoparticles, 30 nm in diameter, 40 wt% dispersed in water.

2.2 Simulation

One of the prime objectives of the multiphase simulation is transient prediction of the droplet-gas interface position. To meet this objective, Eulerian interface capturing method, Volume of Fluid (VOF) is employed to handle the transport of the phases. The volume fraction continuity equation is discretized implicitly in time and the interface advection is discretized by the compressive numerical scheme. All the transport equations are discretized by first order implicit scheme. The pertinent numerical model and discretization details are summarized in Table.1.

Table 1. Numerical Models Used in Simulation

Numerical aspect	Solution method
PV coupling	PISO
Gradient	Green Gauss Node based
Pressure	Body force weighted
Momentum, Species, Energy (convective)	Second order upwind
Multiphase	VOF (Compressive)
Turbulence	SST k-w (Single phase simulation)

A single-phase droplet modeling approach, based on the work of Buongiorno [10], will be used to capture the fluid dynamics of an oscillating nanofluid droplet. An additional scalar equation, shown in Eq. (2) will be solved for volume fraction of nanoparticle (α_{np}) with cell-wise nanofluid properties updated based on relative volume fractions of liquid (α_f) and particles (α_{np}). For the property of nanofluid, appropriate empirical equations were chosen from the compilation provided in the work of Mahian et. al [9]. For turbulence, the normalized pipe wall cell distance Y^+ is ensured to be in the order of ~1. In multiphase simulations, wall serves the purpose of separating the flow boundaries (inlet and outlets), to avoid numerical instability and is assumed to have zero shear. The level of refinement and general structure of the computational mesh for Multiphase domain is adopted from the work of Stefanitsis et. al [10] and Meng et. Al [11], accordingly 50 cPR (cells Per Radius) is ensured for the discretization of the droplet region. The single- phase simulation is conducted to understand the variation of average velocity and pressure at pipe exit. Using the transient variation of velocity and pressure, derived from single phase simulation, as boundary conditions, the multiphase simulations are conducted on a smaller section of single-

phase computational domain, which significantly reduces the number of mesh points and the ensuing computational load.

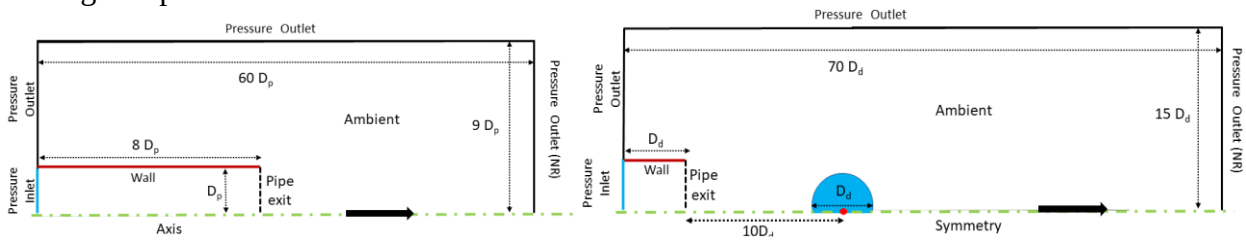

Figure 3. Single phase and Multiphase computational domain

3. Results and Discussion

3.1 Experimental results

Figure 4 shows Schlieren images of the flow leaving the shock tube. A standing wave structure appears to stabilize in the wake of the flow exiting the tube. The structure clearly shows a cross pattern corresponding to intersecting oblique shock waves similar to those seen in overexpanded or underexpanded jets.

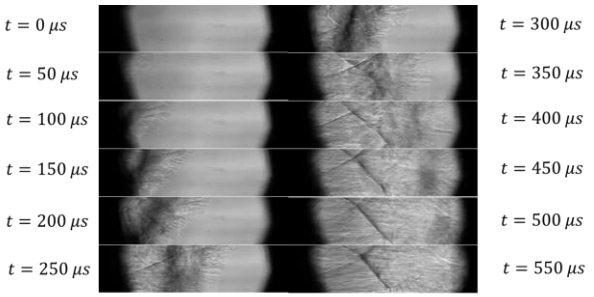

Figure 4. Gas dynamics at tube exit.

When the flow leaving the tube interacts with a droplet, the presence of the droplet is felt by the flow as visualized through a bow-shock like structure formed at the leading edge of the droplet. While the bow shock does not persist at later times, the standing wave structure observed in the gas phase flow in Fig. 4 is seen to be generated even in the case of the flow interaction with the droplet. Figure 5 shows this effect where images obtained from direct and Schlieren imaging are presented. In both images, the droplet can be seen spreading in the downstream direction as the flow strips the droplet leaving thin bags or ligaments of water at the leading edge and generating a finer spray at the trailing edge.

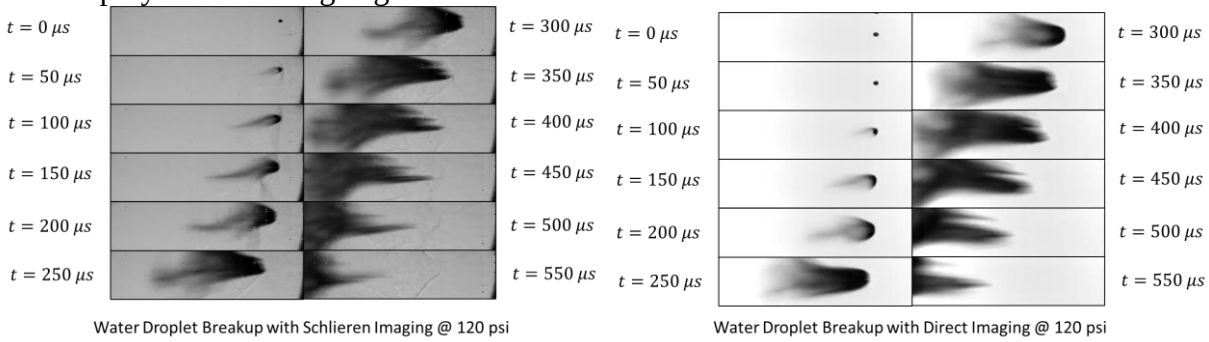

Figure 5. Schlieren images of droplet breakup (Left); direct images of droplet breakup (Right).

Figure 6 shows the effect of varying upstream air pressure which should have a direct influence on the flow velocity. Increasing pressure is observed to narrow the spread of the droplet in the vertical direction, causing a more elongated breakup. At the highest tested pressure of 120 psi, more of the broken-up droplet is seen to persist for a comparable amount of time relative to that seen at 100 or 110 psi. This could indicate that increasing pressure causes an increase in the droplet stripping effect as compared to lower pressures where the droplet mass is simply blown away.

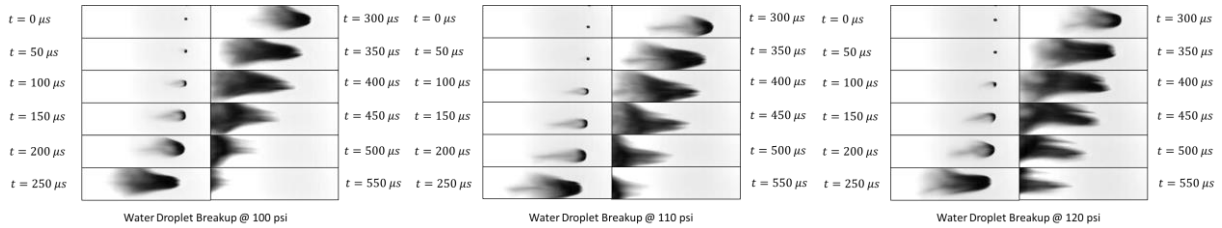

Figure 6. Comparison of droplet breakup at 100, 110 and 120 psi

Figure 7 shows a comparison of the droplet breakup processes for water, and the two nanofluids, Alumina and Titanium dioxide for the same upstream pressure conditiosn. The wake generated in the water droplet appears to be darker than that seen in the case of 20 weight% Alumina which itself appears darker than that for the case of 40 weight % Titanium dioxide. This potentially indicates that the presence of nanoparticles could positively impact the breakup process, accelerating the same, and where an increase in nanoparticle concentration can lead to further enhancement of the breakup process.

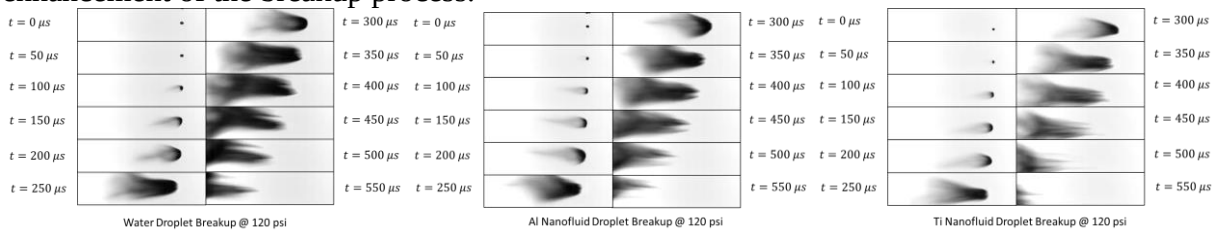

Figure 7. Comparison of droplet breakup with water, Al nanofluids, and Ti nanofluids

3.2 Simulation results

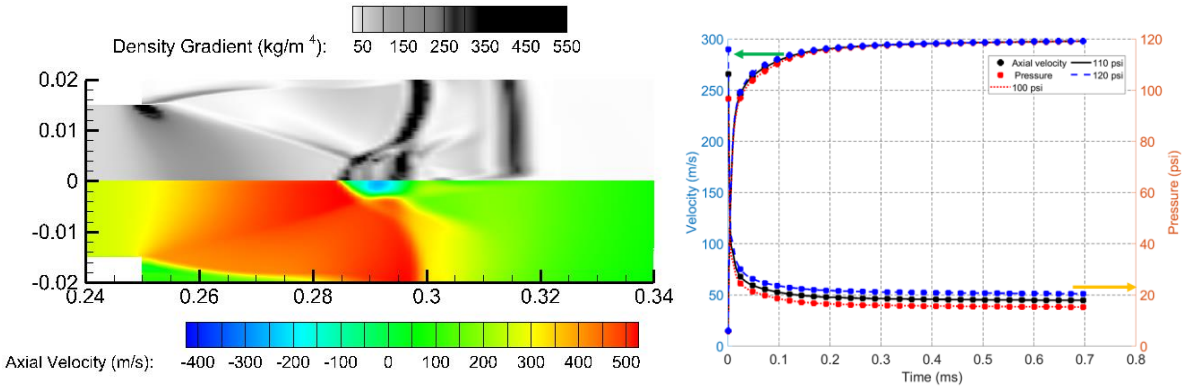

Figure 8. Contour plot showing simulated Schlieren and velocity contours for gas-phase flow at pipe exit (Left) and Transient variation of average velocity and pressure at pipe exit (Right).

Figure 8 shows the simulation results for velocity and pressure at the pipe exit. These values are used for calculations when dealing with the simulated droplet breakup. Figure 8 also shows a contour plot illustrating a simulated Schlieren of the gas phase flow at the exit of the tube. The inclined shock waves observed in the Schlieren images from the experiment shown in Fig. 5 can be observed in the simulation results from Fig. 8.

Figure 9 depicts simulation results of a cylinder of water and nanofluid subject to the high speed flow generated at the tube exit. Flattening of the droplet, vertical stretching, and surface wave generation can be observed. There is recirculation behind the cylinder which is expected to occur. No significant differences are currently observed for the nanofluid case, however this needs to be explored in greater detail. Further, currently only results from early times are available.

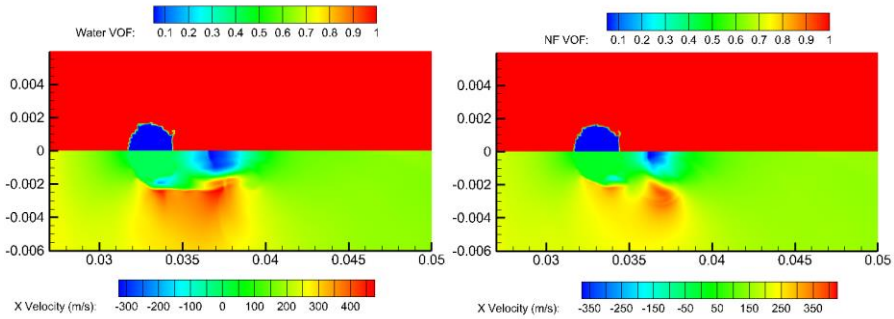

Figure 9. Simulated water droplet (Left) and nanofluid breakup (Right) at 110 psi and 90 μs.

4. Conclusions

High speed impulse flows generated by a pressurized tube were found capable to generate strong breakup of droplets of pure fluids and nanofluids. The breakup process was studied using high-speed imaging approaches. Results indicate that strength of the flow characterized by the initial pressure in the tube influences the droplet mass stripping process. The presence of nanoparticles in the fluid appears to accelerate the droplet breakup process. Preliminary results from multiphase flow simulations appear capable of enabling an improved understanding of the physics underlying the droplet breakup process when exposed to high-speed gas flows.

5. Acknowledgements

This work is supported by NASA EPSCoR and the Board of Regents of the state of Louisiana.

6. References

[1] Zhou, R., Wu, D., & Wang, J. (2015). Progress of continuously rotating detonation engines. Chinese Journal of Aeronautics, Vol 29, 15-29.
[2] Bai, C.-H. , Wang, Y. , Xue, K. , and Wang, L.-F. , “Experimental powder–droplet–vapor mixtures,” Shock Waves, pp. 1–13, 2018.
[3] Salvador, Francisco Javier, and Joaquin Morena. “Scaling Spray Penetration at Supersonic Conditions through Shockwave Analysis.” *Fuel*, vol. 260, 15 Jan. 2020.
[4] Theofanous, T. , “Aerobreakup of newtonian and viscoelastic liquids,” Annual Review of Fluid Mechanics, Vol. 43, pp. 661–690, 2011.
[5] Kauffman, C. , Nicholls, J. , and Olzmann, K. , “The interaction of an incident shockwave with liquid fuel drops,” Combustion Science and Technology, Vol. 3, No. 4, pp. 165–178, 1971.
[6] Faeth, G. M., Hsiang, L. P., & Wu, P. K. (1995). Structure and breakup properties of sprays. International Journal of Multiphase Flow, 21, 99-127.
[7] Karmakar, S., Wang, N., Acharya, S., & Dooley, K. M. (2013). Effects of rare-earth oxide catalysts on the ignition and combustion characteristics of boron nanoparticles. Combustion and flame, 160(12), 3004-3014.
[8] Kannaiyan, K., & Sadr, R. (2017). The effects of alumina nanoparticles as fuel additives on the spray characteristics of gas-to-liquid jet fuels. Experimental Thermal & Fluid Science, 87, 93-103.
[9] Stefanitsis, Dionisis, et al. "Numerical Investigation of the Aerodynamic Droplet Breakup at Mach Numbers Greater Than 1." Journal of Energy Engineering 147.1 (2021): 04020077.
[10] Meng, Jomela C., and Tim Colonius. "Numerical simulation of the aerobreakup of a water droplet." Journal of Fluid Mechanics 835 (2018): 1108-1135.
[11] Mahian, Omid, et al. "Recent advances in modeling and simulation of nanofluid flows-Part I: Fundamentals and theory." Physics reports 790 (2019): 1-48.